QJEGH

Research article

Quarterly Journal of Engineering Geology and Hydrogeology

Published Online First

https://doi.org/10.1144/qjegh2020-073

Electrokinetic-enhanced removal of toluene from physically heterogeneous granular porous media

Richard Thomas Gill*, Steven Thornton, Michael J. Harbottle and Jonathan W. N. Smith

Shell Global Solutions International BV, Rijswijk, South Holland, Netherlands

RTG, 0000-0003-4667-0897; ST, 0000-0002-0235-1600; MJH, 0000-0002-6443-5340; JWNS, 0000-0002-6568-842X

* Correspondence: Richard-Thomas.Gill@shell.com

Abstract: Electrokinetics (EK) was applied to enhance biodegradation of toluene in the low hydraulic conductivity (*K*) zone of a physically heterogeneous water-saturated granular porous media. The hypothesis tested was that EK transport processes, which operate independently of advection, can deliver a limiting amendment, nitrate, across a high-*K*–low-*K* boundary to stimulate bioremediation. Two types of experiment were evaluated: (1) bench-scale tests that represented the active EK system and physically heterogeneous sediment configuration; (2) microcosms that represented biodegradation in the bench-scale tests under ideal conditions. The bench-scale experiment results showed a rapid decrease in toluene concentration during the application of EK that was attributed to electroosmotic removal from low-*K* zones. Comparison of toluene removal rates by electroosmosis and biodegradation (microcosm) confirmed that electroosmosis was the most effective mechanism under the conditions evaluated. Overall, this work challenges the original hypothesis and indicates that, at the field scale, the most favourable conditions for biodegradation are likely to be achieved by applying EK to increase contaminant flux across the low-*K*–high-*K* boundary (out of the low-*K* zone) and allowing biodegradation to occur in the high-*K* zone either by natural attenuation or enhanced by amendment addition.

Supplementary material: Supplementary material is available at https://doi.org/10.6084/m9.figshare.c.5174554

Received 14 April 2020; **revised** 10 August 2020; **accepted** 10 October 2020

Contamination of physically heterogeneous aquifers (where hydraulic conductivity (*K*) varies) can present a long-term environmental management challenge. In these settings, contaminants can become sequestered in low-*K* zones and persist as secondary sources of groundwater contamination over long time periods. This occurs as a result of the presence of concentration gradients across the interface between the low-*K* zone and high-*K* host matrix that initially drives diffusion into the low-*K* zone. This concentration gradient is later reversed after advection of contaminants from the high-*K* host matrix, resulting in 'back-diffusion' of contaminants out of the low-*K* zone (Tatti *et al.* 2018). Electrokinetic-enhanced bioremediation (EK-BIO) is a promising solution to this technical problem. Electrokinetics (EK) is the application of a direct current to the subsurface to initiate certain transport phenomena independent of *K*, such as electromigration (movement of dissolved ions) and electroosmosis (movement of pore fluid) (Gill *et al.* 2014). In theory, EK transport phenomena can be used to enhance mass transfer of amendments across *K* boundaries to stimulate bioremediation in a low-*K* zone and reduce contaminant mass by removal (Reynolds *et al.* 2008; Gill *et al.* 2015). However, application of EK-enhanced bioremediation represents a complex mix of processes, the contributions of which may influence remediation performance. For example, if electromigration of the amendment is too low owing to a low voltage gradient (Wu *et al.* 2012*a*) or variation in the sediment properties (Gill *et al.* 2015), then the delivery rate may not be sufficient to meet the oxidant demand from biodegradation (Rabbi *et al.* 2000). Alternatively, the electroosmotic pore fluid flux may be too high, shifting the zone of anticipated biodegradation further into the high-*K* zone. More studies are required to understand the mechanisms controlling EK-BIO in physically heterogeneous settings, to develop technically appropriate and cost-effective treatment strategies.

Previous EK-BIO studies have been conducted in physically homogeneous settings (Mao *et al.* 2012; Huang *et al.* 2013; Hansen *et al.* 2015). Many sediment types and properties have been evaluated in these studies, from high-*K* sands (Luo *et al.* 2005) to low-*K* clays (Wu *et al.* 2012*c*). The effectiveness of EK in introducing amendments into physically heterogeneous aquifers has been demonstrated at the laboratory scale (Reynolds *et al.* 2008) and modelled field scale (Wu *et al.* 2012*a*). Gill *et al.* (2015, 2016*a*) expanded these findings by demonstrating a connection between spatial variation in material properties and voltage gradient to highlight the controls on amendment transport in heterogeneous systems. Currently, there are no published laboratory studies that apply EK-BIO in physically heterogeneous settings. This is an important research gap because most aquifers are physically heterogeneous with respect to *K* distribution and a principal advantage of EK is its effectiveness across a range of *K* values, when combined with other techniques such as bioremediation. The aim of the research presented in this paper was to investigate the relative impacts of EK on nitrate delivery, toluene (herein used as a model oxidizable organic compound) transport and biodegradation of toluene initially located in a low-*K* zone. The hypothesis tested was that EK transport phenomena (namely electromigration) should enhance the biodegradation of toluene over advection by increasing the supply of nitrate to toluene in the low-*K* zone. As delivery of oxidant amendments into low-*K* zones of hydrocarbon-contaminated aquifers is a potential limitation of conventional remediation methods, such as engineered bioremediation (Thornton *et al.* 2016), this scenario explores the relative impact of EK on nitrate delivery, toluene transport and biodegradation potential in a relevant physically heterogeneous setting.

Materials and methods

Experimental design

Two types of experiment were used to address the research aim: (1) bench-scale experiments using the test rigs developed by Gill *et al.*

Table 1. *Experimental variables applied to each test rig during the bench-scale experiments*

Test rig designation	Inoculum	Nitrate	EK
A	✗	✓	✓
B	✓	✓	✗
C	✓	✗	✓
D	✓	✓	✓

(2015, 2016*a*); (2) microcosm experiments. Both approaches used the same sediment materials, toluene and inoculum. The bench-scale experiments were designed to initiate biodegradation in low-*K* zones following the addition of nitrate by electromigration. Three different controls were used, which exclude the inoculum, nitrate amendment and voltage gradient (i.e. the presence of 'EK') from the setup (Table 1). All bench-scale experiments comprised a physically heterogeneous sediment configuration, with a high-*K* material arranged adjacent to a low-*K* material, a dissolved toluene source and pH control. The microcosm experiments were performed to independently confirm the potential for toluene biodegradation by the inoculum using nitrate as an oxidant under ideal conditions. The experiment was run for 16 days to accommodate amendment transport and allow sufficient time for microbial degradation of toluene.

Material and contaminant properties

Two types of silica sand were used to represent high- and low-*K* material: (1) a coarse-grained sand (David Ball Group Ltd); (2) a fine-grained sand (Marchington Stone Ltd) mixed 80:20 by weight with kaolin clay (Speswhite, Imerys Performance Materials Ltd) to reduce the *K*-value. Table 2 shows the grain size distribution of these materials. Prior to the experiment the sediment was sterilized to minimize biological contamination. The sterilization method used depended on the material. Coarse-grained sand was autoclaved twice and the fine-grained sand and kaolin mix was heat sterilized (3 h at 150°C). Autoclaving clays can cause aggregation and occlusion of pore spaces, whereas these effects are less pronounced for heat sterilization (Jenneman *et al.* 1986). This phenomenon could influence EK migration of substances in the experiment; hence heat sterilization was used. The electroosmotic permeability value reported in Table 2 is taken from experiments using the same material (Gill *et al.* 2015); information on how the value was calculated have been provided by Gill (2016).

Table 2. *Physical properties of sediment used in the experiments*

Material property (units)	High-*K*	Low-*K*
Grain size (mm)	Fraction (%)	Fraction (%)
<4–2	1.02	0
<2–1	98.75	0
<1–0.5	0.20	0.34
<0.5–0.1	0.02	80.65
<0.1–0.05		3.97
<0.05–0.01		4.24
<0.01–0.005		5.44
<0.005–0.001		3.72
<0.001–0.005		0.42
<0.005–0.0001		1.06
Fraction of organic carbon, f_{oc}* (–)	0.0015	0.0016
Porosity (–)	0.39	0.39
Hydraulic conductivity, K (m s^{-1})	7.0×10^{-4}	6.6×10^{-9}
Electroosmotic permeability, K_e (m^2 V^{-1} s^{-1})	–	3.8×10^{-9}

*Method from the British Standard Institute (1990).

Toluene was selected for these experiments because it is a common component in petroleum light non-aqueous phase liquid (LNAPL) contaminants (CL:AIRE 2014), frequently considered a constituent of potential concern at LNAPL release sites (Bowers and Smith 2014), but is less hazardous to work with than other compounds, such as benzene. It is a representative oxidizable compound that is readily biodegraded in the environment by both aerobic and anaerobic pathways. However, because petroleum releases frequently create anaerobic conditions *in situ*, in which denitrification is an important biodegradation process, nitrate was used as a model electron acceptor (Rivett *et al.* 2008). Toluene can be degraded by the selected inoculum at a concentration equivalent to 46 mg l^{-1} (Lavanchy 2008), which is comparable with the theoretical maximum dissolved concentration found in source zones at LNAPL release sites.

Inoculum properties

Thauera aromatica was selected as the inoculum for these experiments (DSMZ Ltd, Germany, No. 6984). It is well documented in the literature with the ability to degrade toluene under denitrifying conditions using nitrate as a terminal electron acceptor (Anders *et al.* 1995). It is a facultative anaerobe, although the toluene-degrading function of *T. aromatica* is reported to be sensitive to aerobic conditions and will cease when the nutrient medium is saturated with dissolved oxygen (Lavanchy 2008). Preliminary tests confirmed anaerobic growth of *T. aromatica* on defined media (Table 3) using toluene and nitrate as a carbon source and electron acceptor, respectively (Supplementary material, Section S.1.1).

A synthetic groundwater was used in the bench-scale and microcosm experiments, consisting of a dilute solution (five-times dilution) of the defined media. The electrical conductivity of the synthetic groundwater (819 µS cm^{-1}) was equivalent to that of typical groundwater (Thornton *et al.* 1995) and in previous similar experiments (Gill *et al.* 2015, 2016*a*). The ability of the synthetic groundwater to support *T. aromatica* growth was confirmed using microcosms prior to setting up the bench-scale experiment.

Bench-scale experimental setup

The bench-scale rigs were the same as those described by Gill *et al.* (2015, 2016*a*), with some minor modifications (Fig. 1). The sediment and individual electrode chamber volumes were 7.5 l and 2 l, respectively. Physical heterogeneity in the experiment was represented by two materials with different *K* values, using the same configuration as described by Gill *et al.* (2015). However, a different consolidation process was applied to account for the use of an anaerobic inoculum. A thin (0.5 mm) plate was used to divide the

Table 3. *Solutions used to grow T. aromatica*

Defined media		Synthetic groundwater	
	Solution A		Solution A
1.63 g l^{-1}	KH_2PO_4	0.33 g l^{-1}	KH_2PO_4
11.8 g l^{-1}	K_2HPO_4	2.37 g l^{-1}	K_2HPO_4
	Solution B		Solution B
1.06 g l^{-1}	NH_4Cl	0.21 g l^{-1}	NH_4Cl
0.4 g l^{-1}	$MgSO_4.7H_2O$	0.08 g l^{-1}	$MgSO_4.7H_2O$
4 g l^{-1}	KNO_3	0.8 g l^{-1}	KNO_3
0.05 g l^{-1}	$CaCl_2.2H_2O$	0.01 g l^{-1}	$CaCl_2.2H_2O$
10 ml l^{-1}	Trace elements*	2 ml l^{-1}	Trace elements*
5 ml l^{-1}	Vitamin solution*	1 ml l^{-1}	Vitamin solution*

Solutions A and B were autoclaved separately and combined after cooling.
*See Supplementary material, Section S.1.2 for component list.

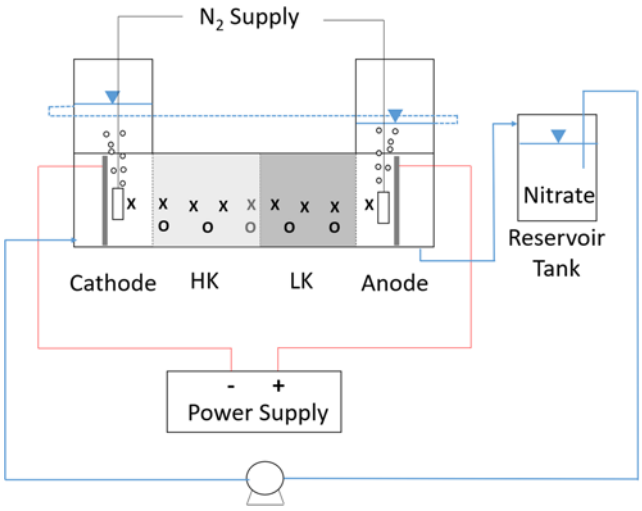

Fig. 1. Schematic illustration of test cell design showing sediment chamber with high- and low-*K* zones (HK and LK, respectively), voltage probes (O) and sampling ports (X). The power supply to electrodes, nitrate amendment supply and nitrogen sparge apparatus are also shown.

sediment chamber during consolidation. High-*K* sediment material was added to the high-*K* compartment and consolidated using the shaker table method (Supplementary material, Section S.1.3). Once the high-*K* material was consolidated within the rig it was transferred to an anaerobic chamber with a tray containing the sterilized fine-grained sand and kaolin mix. The fine-grained sand and kaolin mix was then wetted with a volume of degassed synthetic groundwater (30% of the kaolin fraction volume). Two different solutions of the same synthetic groundwater were added to the sand kaolin mix: (1) the majority, 900 ml (or 90%) contained the inoculum (Supplementary material, Section S.1.4); (2) a concentrated toluene stock, 100 ml (Supplementary material, Section S.1.5). At the beginning of the experiments, the low-*K* zone was at 30% saturation and the average starting toluene concentration was 16 mg l^{-1}. The wetted fine-grained sand and kaolin mix was then added to the low-*K* compartment in layers *c.* 3 cm thick and tamped down using a ceramic pestle. This method ensured the inoculum was evenly distributed through the low-*K* zone. The cell count of the synthetic groundwater containing the inoculum was 9.8×10^5 ($\pm 4.5 \times 10^5$) cells ml^{-1} based on microscopic analysis. The blank (control) rig was also prepared using the same volume of water and sediment as the other rigs, but the inoculum was not included.

Once the material was consolidated and the lid secured, the rig was removed from the anaerobic chamber. It was then connected to two carboys: (1) a 20 l carboy containing sterile (autoclaved), degassed synthetic groundwater; (2) a 10 l carboy containing synthetic groundwater and the inoculum (Supplementary material, Section S.1.4). The 10 l carboy was connected to the valve at the base of the high-*K* section and the 20 l carboy to the valves in the base of the electrode chambers. Synthetic groundwater was removed from the carboys by displacing it with nitrogen gas, to ensure fluid entering the base unit was anaerobic. Before the addition of synthetic groundwater the carboys were sterilized using bleach and rinsed with sterilized UHQ water. During this process the header tanks were put in place and filled to the desired levels. The high-*K* section was considered saturated once fluid was observed emerging from threaded ports in the base unit lid; these were then sealed. After saturation the high-*K* zone was assumed to have inoculum evenly distributed within it. The electrode chambers were filled with synthetic groundwater; once the level was above the height of the sediment chamber, the rigs were connected to the nitrogen sparge system. This consisted of a nitrogen line into each electrode chamber that bubbled nitrogen through the electrolyte. The objective was to remove oxygen that could either diffuse into the sediment chamber or be transported with the electroosmotic pore fluid flux from the anode. Once the system was connected, it stood with only the nitrogen sparge active for 24 h to ensure anaerobic conditions and to allow microbial attachment to the sediment this is analogous to similar experiments performed by Song and Seagren (2008).

A direct current was applied at a constant current of 25 mA (1.6 A m^{-2}) from a power pack (Digimess, PM6003-3). A recirculation system with a pump rate of 25 ml min^{-1} was applied to neutralize the fluid pH in these experiments. The configuration of the recirculation system was similar to those used by Wu *et al.* (2012*c*) and Mao *et al.* (2012), where a cross circulation tube transfers the catholyte fluid to the anode. However, unlike these methods, the head difference between electrodes allows fluid transfer between electrodes without the need for an additional pump or the risk of short-circuiting the sediment chamber. The head difference is equivalent to a hydraulic gradient of 0.14 between the electrode chambers and provides an advective flux three orders of magnitude lower than the fluid flux achieved by electromigration (Supplementary material, Section S.1.6). Thus, the advective flux is considered to be negligible during the experiment.

Microcosm experimental setup

Microcosms were designed to mimic biodegradation processes occurring within the EK test cells. A series of blank microcosms without inoculum represented the control. In total 54 sacrificial microcosms (each 20 ml vials) were prepared. These included active and control systems, which were destructively sampled in triplicate at nine time points including t_0, over a period of 18 days. The microcosm preparation included the following steps: (1) sterilization of vials, caps and other relevant apparatus by autoclave; (2) transfer of apparatus, sterilized sediment and degassed synthetic groundwater to an anaerobic chamber; (3) transfer of a 6.3 ml aliquot of the synthetic groundwater to a vial (synthetic groundwater for control microcosms was filter sterilized (0.22 µm pore size) before addition); (4) addition of 25 g sediment to the vial by pluviation; (5) addition of 0.1 ml aliquot of 1M NaOH to raise the pH from pH 5 to pH 7 and capping; (6) degassing of vials through the cap; (7) addition of 0.54 ml of toluene solution (600 mg l^{-1}) to the vial through the cap to achieve a final concentration of 20 mg l^{-1}; (8) addition of 0.088 ml of KNO_3 solution (150 g l^{-1}) through the vial cap 4 days later, after the bacterial attachment phase. When solutions were added to the vial, it was homogenized using a vortex.

Monitoring and analysis of bench-scale and microcosm experiments

In bench-scale tests each test cell had seven fluid sampling points evenly spaced along the sediment chamber, one in each electrode chamber and one for the reservoir tank (Fig. 1). Fluid samples were taken every 48 h. Sampling tubes were made of PEEK plastic and a sintered glass block was fitted to the end of individual tubes to prevent blockage by sediment. Five voltage probes were inserted into the sediment. Voltage and current readings were measured daily using a multimeter (Digitek, DT-4000ZC), when a direct current was applied to the sediment. In microcosm experiments fluid samples were collected by removing the vial cap and inserting a sampling tube with a sintered glass block. Once a fluid sample was extracted it was transferred to a glass vial for chemical analysis.

Fluid samples were analysed for major ion and toluene concentrations. Major ions were analysed using an ion chromatograph (Dionex ICS 3000, Thermo Scientific). Toluene analysis was conducted on a Varian gas chromatograph (CP-3800) with an

attached Varian mass spectrometer (Saturn 2000). Samples for toluene analysis were extracted from vials using a solid-phase microextraction autosampler. For both the Dionex and gas chromatography–mass spectrometry (GC–MS) method a five-point calibration was included in each run and quality control standards were included within the sample suite. A 7.5 µl aliquot of internal standard containing 101.5 mg l^{-1} deuterated toluene was added to each sample for GC–MS analysis. pH was measured in selected pore fluid samples.

Results and discussion

Conceptual model of bench-scale experiment

Toluene transport and mass removal from the low-*K* zone in the bench-scale experiments can occur by several mechanisms; namely, electroosmosis, diffusion, sorption and biodegradation. The influence and general characteristics of these processes are shown in a conceptual model in Figure 2. Electroosmotic flow moves pore fluid from the anode to the cathode, providing a transport vector for dissolved toluene from the low-*K* to high-*K* zone and into the cathode chamber. Mass flux by electroosmosis of a solute (i.e. toluene) *i*, J_i^{eo}, is given by (Acar and Alshawabkeh 1993)

$$J_i^{eo} = C_i v_i^{eo} \tag{1}$$

where J_i^{eo} is the electroosmotic mass flux (mg m^{-2} s^{-1}), C_i is the solute concentration in the pore fluid (mg m^{-3}) and v_i^{eo} is the solute velocity under the electroosmotic pore fluid flux (m s^{-1}). The solute transport velocity will be a function of the retardation factor:

$$R_f = \frac{v_w}{v_i} = \frac{v_w^{eo}}{v_i^{eo}} \tag{2}$$

where R_f is the solute retardation factor, v_w is the pore fluid flux (m s^{-1}) v_i is the solute velocity (m s^{-1}) (Hiscock 2005) and v_w^{eo} is the pore fluid velocity by electroosmosis, described by

$$v_w^{eo} = k_e \frac{\partial E}{\partial x} \tag{3}$$

where k_e is the electroosmotic permeability (m^2 V s^{-1}), *E* is the electrical potential (V) and *x* is distance (m). The retardation factor accounts for sorption of the toluene to the sediment, which influences the contaminant transport velocity by electroosmosis (Bruell *et al.* 1992). The retardation factor is determined by the partition coefficient, K_d (ml g^{-1}), of the contaminant between the pore fluid and sediment (Fetter 2001):

$$R = 1 + \frac{\rho_b}{n} K_d. \tag{4}$$

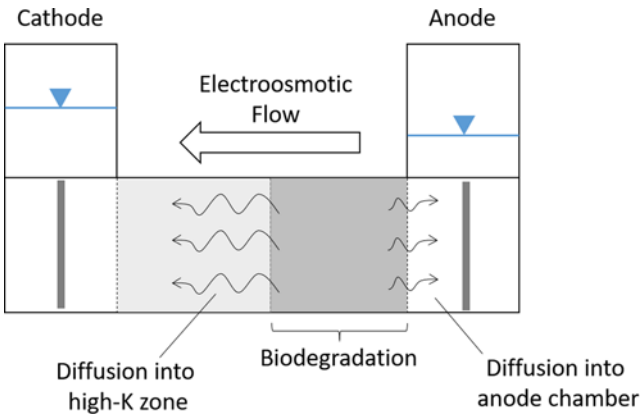

Fig. 2. Conceptual model for toluene mass removal processes occurring in the bench-scale experiments.

where ρ_b, is the bulk density (g mL^{-1}); and *n*, porosity (–). The K_d value is in turn a function of the sediment fraction of organic carbon, f_{OC}, and can be estimated according to the following relationship for organic compounds with a water solubility $<1 \times 10^{-3}$M (Delle Site 2001):

$$K_{OC} = \frac{K_d}{f_{OC}} \tag{5}$$

where K_{OC} is the normalized partition coefficient of the solute onto organic carbon (ml g^{-1}). In the experiment retardation of toluene is expected to occur owing to the organic carbon content of the sediment (Table 2).

Solute diffusion is described by the diffusion mass flux equation:

$$J_i^D = -D_i^* \frac{\partial C_i}{\partial x} \tag{6}$$

where J_i^D is the diffusive mass flux (mg m^{-2} s^{-1}) and D_i^* is the effective diffusion coefficient for a solute *i*. Solute diffusion will occur across the low-*K*–high-*K* and low-*K*–anode chamber interface. The diffusion rate is expected to be higher at the low-*K*–anode chamber interface for the following reasons: (1) toluene diffuses into a fluid chamber in which the diffusion coefficient at infinite dilution applies, whereas across the low-*K*–high-*K* interface it is a function of the tortuosity of the high-*K* material; (2) a higher concentration gradient exists because toluene is assumed to be removed quickly from the anode chamber by volatilization owing to nitrogen sparging, adsorption onto the graphite electrode and the recirculation system.

Biodegradation of toluene by *T. aromatica* is expected to occur via denitrification, as observed in the preliminary growth experiments. The first step is reduction of nitrate to nitrite, which is then ultimately reduced to nitrogen gas (Anders *et al.* 1995):

nitrate reduction to nitrite:

$$C_7H_8 + 18NO_3^- \rightarrow 18NO_2^- + 7CO_2 + 4H_2O \tag{7}$$

nitrite reduction to nitrogen:

$$C_7H_8 + 18NO_2^- \rightarrow 7N_2 + 7CO_2 + 4H_2O. \tag{8}$$

Based on these relationships toluene biodegradation can be indirectly monitored by changes in the pore fluid nitrate and nitrite concentration. Biodegradation was anticipated to occur in the low-*K* zone owing to the high concentration of nitrate and toluene and presence of microbes.

Toluene can potentially be adsorbed onto the bench-scale rig components. Adsorption tests were conducted on two key materials used in the rigs: (1) acrylic, used to construct the base unit and header tanks; (2) the rubber gasket used to prevent leaks at the interface between the base unit, lid and header tanks. The method and results for these tests are presented in the Supplementary material, Section S.2.1. The results show that there was minimal adsorption of toluene to acrylic compared with the control vial, which contained no rig components. Conversely, the rubber gasket adsorbed >50% of the toluene over 72 h, at which point it had reached equilibrium. The bench-scale rigs stood for 24 h before baseline sampling. To simplify the conceptual model, it was assumed that the change in toluene concentration owing to sorption to the gasket was negligible at the time of baseline sampling based on the sorption test.

*Removal of toluene from low-***K** *zone by electroosmosis*

A direct current was applied to Rigs A, C and D for 96 h. This accounts for the time required (1) for nitrate to migrate into the sediment chamber and low-*K* zone by electromigration from the cathode and (2) to prevent full removal of toluene out of the low-*K* zone by the

electroosmotic pore fluid flux. After this period the current was switched off to allow the inoculum sufficient time to degrade toluene.

The toluene concentration in the low-*K* zone of the different rigs is shown in Figure 3. These values were derived from the sum of toluene mass in the low-*K* zone divided by the pore fluid volume of the low-*K* zone. The toluene mass was obtained from integration of the pore fluid concentration over the dimensions of each bench-scale rig. The toluene mass values for the low-*K* zone were then summed and divided by the pore fluid volume of the low-*K* zone. The toluene concentration for each rig decreased over time owing to different removal mechanisms (Fig. 3). In the rigs where EK is applied (cells A, C and D) there is a rapid decrease in toluene concentration in the low-*K* zone during the period when a direct current was applied. In Rig A this effect is delayed. Only in Rig B, the no-EK control, was a sharp decrease in toluene concentration not observed within the test cell, implying that the phenomenon was associated with the application of EK. Furthermore, in experiments where EK was applied, toluene was found in the high-*K* zone (Supplementary material, Figure S.4), but this was not the case in the no-EK experiment. The conceptual model suggests that toluene migration by electroosmotic flow will be predominantly towards the cathode (Fig. 2), hence toluene should be detected in the high-*K* zone under the influence of EK. This indicates that electroosmotic flow is the principal mechanism for toluene removal from the low-*K* zone during the period EK was applied.

After the bench-scale experiments a further test was conducted to demonstrate the influence of electroosmotic flow on toluene removal. The application of direct current was swapped between Rig B (no EK) and Rig C (nitrate control, EK applied). Results presented in the Supplementary material (Figure S.5) showed that when a direct current was applied, the toluene concentration rapidly decreased compared with a no-EK system, where the toluene concentration persisted.

*Removal of toluene from low-*K *zone by biodegradation*

Toluene removal by biodegradation under ideal conditions is shown in the microcosm experiment (Fig. 4). There are two observations that indicate that the decrease in toluene concentrations in the active microcosm resulted from biodegradation by denitrification. First, when the nitrate solution was added after 96 h there was a greater decrease in the toluene concentration in the active microcosm relative to the control (Fig. 4); second, there was a corresponding increase in nitrite concentrations (Fig. 5). The decrease in toluene concentrations within the control microcosm is unlikely to result from biodegradation. This is evidenced by the stoichiometric relationship (equation 7) where the increase in nitrite concentration

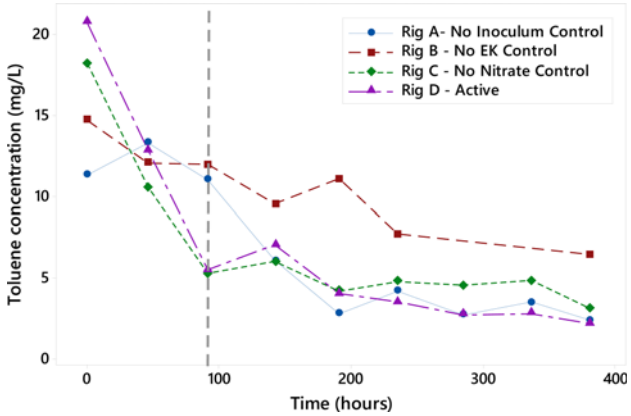

Fig. 3. Toluene concentration in the low-*K* zone for the different bench-scale rigs. The dashed line indicates when the direct current was switched off in Rigs A, C and D.

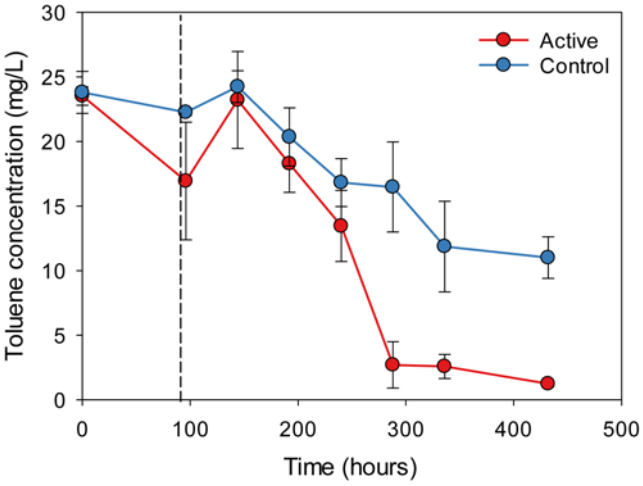

Fig. 4. Toluene concentration in the active and control microcosm. The dashed line at $t = 96$ h indicates when the nitrate solution was added.

(maximum 20.4 mg l^{-1}) is equivalent to transformation of 2.3 mg l^{-1} toluene, which is less than the 9.5 mg l^{-1} decrease observed in Figure 4. Abiotic toluene loss from the microcosms could arise from the vial cap being compromised during the addition of the concentrated nitrate solution. However, the additional removal of toluene from the active microcosm in excess of the control microcosm is considered to reflect evidence of biodegradation.

Toluene biodegradation could not be deduced in the bench-scale experiments from any changes in the pore fluid chemistry similar to those recorded in the microcosm experiments. However, there was slow removal of toluene in the rigs after the application of EK and a minimal difference between the active and no-inoculum control (Rig D and A, respectively; Fig. 3). Moreover, it is difficult to identify a change in the nitrate concentration indicative of biodegradation (Fig. 6). The nitrate consumption predicted from toluene biodegradation (post electroosmotic flux) is less than the 5% analytical precision of the nitrate measurement. Nitrite was present in all bench-scale experiments (Fig. 6) but there were no evident increases in concentration in the active system (Rig D), relative to the other rigs, to suggest that biodegradation was occurring as in the microcosm experiment (Fig. 5). The production of nitrite in the no-inoculum control rig and microcosm control indicates the presence of bacteria and evidence of denitrification.

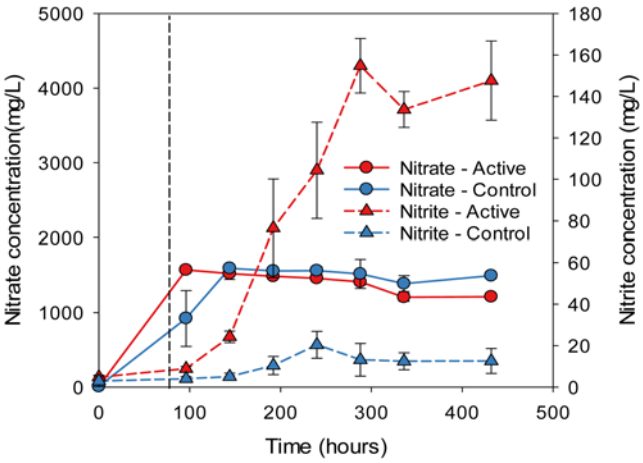

Fig. 5. Nitrate and nitrite concentrations for the microcosm experiments. The dashed line at 96 h indicates when the concentrated nitrate solution was added.

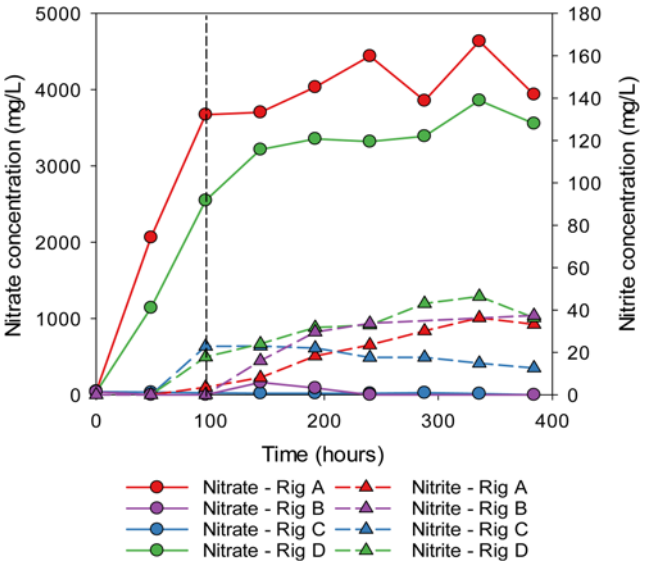

Fig. 6. Nitrate and nitrite concentrations in the low-*K* zone within the bench-scale experiment. The dashed line indicates when EK is switched off. The nitrate concentration in Rig B accounts for sample draw from the high-*K* zone.

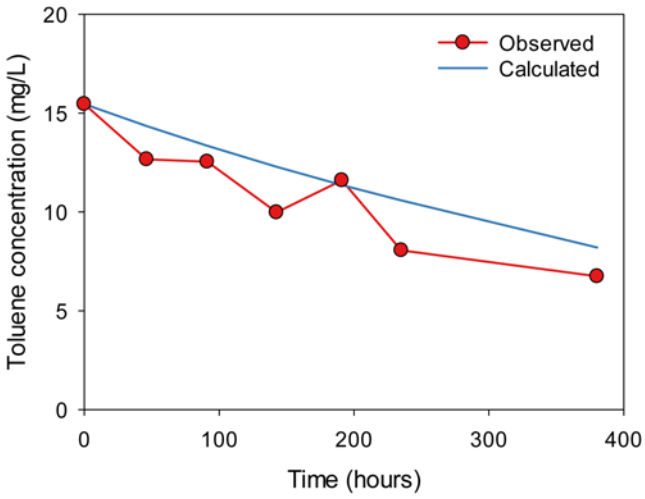

Fig. 7. Observed and calculated toluene concentrations for the low-*K* zone in no-EK control, Rig B. The calculated concentration represents toluene loss by diffusion only.

Nitrite in the no-nitrate control is probably due to denitrification of residual nitrate from the pelleting process.

Nitrite in the no-inoculum and no-nitrate controls is unlikely to arise from biodegradation of toluene. First, the stoichiometry between nitrite production and toluene consumption observed in the active microcosm is not repeated. Second, growth tests of *T. aromatica* using synthetic groundwater demonstrated no growth on a toluene substrate when the nitrate concentration was <59 mg l^{-1}. Overall, this suggests that the nitrite observed in the no-inoculum and no-nitrate controls was due to denitrification of an alternative carbon source to toluene. Additional carbon sources that could account for the increase in nitrite include the dilute vitamin solution (3.4 mg l^{-1}; Supplementary material Table S.1) and particulate organic carbon in the sediment (2.7 mg kg^{-1}; Table 2). Further analysis confirmed that the nitrite produced in the bench-scale rigs could arise from these alternative carbon sources (Supplementary material, Section S.2.3). Overall, the active system could not be differentiated from the no-inoculum and no-nitrate control, therefore enhanced biodegradation of nitrate could not be confirmed. An assessment of potential limitations to enhanced bioremediation in the bench-scale experiments is provided in the Supplementary material, Section S.2.4. It was concluded that a low phosphate concentration could limit toluene biodegradation.

*Removal of toluene from low-*K *zone by diffusion*

Diffusion is expected to be an important process in the bench-scale experiments, according to the contrast in *K* properties of the media. However, it was difficult to observe direct evidence of diffusion because the main diffusion pathway was into the anode chamber. No toluene was detected in the anode chamber and it is expected that any toluene present would have a short residence time owing to the recirculation system, volatilization from the nitrogen sparge and adsorption onto the graphite electrode. Predicted values of the diffusion mass flux out of the low-*K* zone at the low-*K*–anode and low-*K*–high-*K* boundaries can be obtained using equation (6) and the assumptions in Supplementary material, Section 3.1. This calculation is applied to Rig B, where no EK is applied and mass transport by advection is limited (Fig. 7). The results show that a good fit can be obtained between the observed and calculated toluene concentration in the low-*K* zone, implying that diffusion occurred in these systems.

Sensitivity analysis for toluene removal by electroosmosis

Overall, these experiments suggest that the most effective removal mechanism for toluene from the low-*K* zone under the represented conditions was electroosmosis. This process dominated over biodegradation or diffusion and accounted for up to 73% of toluene removed (Fig. 3). A comparison of toluene removal rates from the low-*K* zone is shown in Table 4.

The observation of enhanced organic compound removal by electroosmosis is not new. For example, Bruell *et al.* (1992) demonstrated removal of Benzene, Toluene, Ethylbenzene and Xylene (BTEX) compounds, tetrachloroethene and isooctane from clays by electroosmosis, using water as the purging solution. Furthermore, contaminant removal in physically heterogeneous settings has been documented by Saichek and Reddy (2005), who observed phenanthrene removal from low-*K* zones in different low-*K*–high-*K* configurations. The novel aspect of the work reported here is the comparison of electroosmotic and biodegradation removal rates for an organic compound. It highlights the relationship between toluene removal by electroosmotic pore fluid flux and electromigration of an amendment to enhance biodegradation. This is important for EK-BIO applications in physically heterogeneous settings because this relationship will determine the main removal mechanism and ultimately the efficiency of the treatment. A sensitivity analysis was undertaken to highlight the

Table 4. *Toluene removal rate observed in bench-scale and microcosm experiments*

Removal mechanism	Experiment	Observed removal rate (mg l^{-1} h^{-1})
Electroosmosis (+ diffusion)	Rig A	0.10
	Rig B*	0.079
	Rig C	0.15
	Rig D	0.18
Diffusion	Rig B	0.023
	Rig C*	0.008
Biodegradation	Microcosm†	0.066

*Toluene mass removal rate following EK application to Rig B and no-EK application to Rig C (see Supplementary material).
†Data account for the toluene loss observed in the control microcosm.

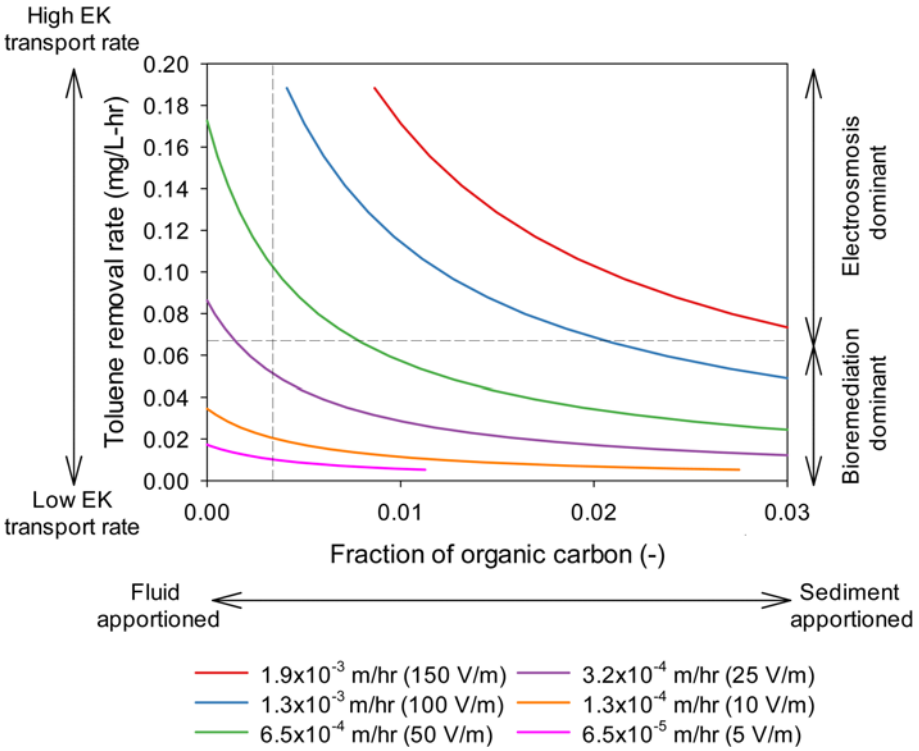

Fig. 8. Sensitivity analysis of toluene removal to different system variables. The different data series represent the toluene removal rate at different electroosmotic flow rates (m h^{-1}) and voltage gradients (V m^{-1}). The dashed lines intercepting the *y*- and *x*-axis represent the toluene removal rate by biodegradation and the experimental f_{OC} value.

factors controlling toluene removal by electroosmosis and to identify the experimental conditions under which stimulating biodegradation would become the dominant toluene removal process in the low-*K* zone. The analysis is shown in Figure 8 where toluene removal rate by electroosmosis is plotted against the sediment f_{OC}. The f_{OC} is back calculated using equations (1)–(5) and the parameters shown in Table 2. The range of f_{OC} values is typical of those observed in the soil or geological environment, <0.01 to 0.03 (Hiscock 2005). The data series represent the toluene removal rate at different electroosmotic pore fluid velocities. These are calculated from equation (1) using the experimental electroosmotic permeability, k_e, value (Table 2) and a range of voltage gradients (1.5–0.5 V m^{-1}). The experimental values for toluene removal by biodegradation and sediment f_{OC} are shown by the dashed lines intercepting the *y*- and *x*-axis respectively. The biodegradation rate is considered at its upper limit because the microcosms were conducted under optimal conditions.

In the context of these experiments the sensitivity analysis shows that the electroosmostic pore fluid velocity must decrease for biodegradation to be the dominant removal mechanism. Within the confines of the experimental parameters already discussed, reduction of the electroosmotic pore fluid velocity is achieved by lowering the voltage gradient. It would need to decrease to *c.* 25 V m^{-1} to generate an electroosmotic pore fluid velocity of 3.2×10^{-4} m h^{-1}, equivalent to a toluene removal rate below 0.066 mg l^{-1} h^{-1}. A low voltage gradient is representative of systems where a constant current is applied and an ionic amendment is added, which will increase the electrical conductivity of the sediment pore fluid (Wu *et al.* 2012*b*). This leads to a decrease in the voltage gradient over time. In these experiments the voltage gradient in Rig D dropped from 72 to 19 V m^{-1} over 91 h of EK application. In addition, the influence of physical heterogeneity may also affect the distribution of the voltage gradient. Gill *et al.* (2015) observed that in physically heterogeneous settings materials with a low effective ionic mobility corresponded to zones with a high voltage gradient. This is shown in Figure 9 for Rig D where the voltage gradient profile (normalized to the voltage between electrodes) is higher across the low-*K* material compared with the high-*K* material. A similar effect was observed in Rig A and Rig C but is less consistent. This effect of heterogeneity could create an enhanced electroosmotic fluid flux across the low-*K* zone, leading to greater contaminant removal compared with homogeneous settings in these experiments.

In the broader context of EK-BIO applications in systems with different properties, a variation in k_e and f_{OC} would change the proportion of contaminant removal by biodegradation and electroosmosis. First, sediment with a high k_e and subsequent high electroosmotic pore fluid flux is advantageous for contaminant removal but can hinder EK-BIO applications. The k_e in these experiments is 3.7×10^{-9} m^2 V^{-1} s^{-1} (Table 2), similar to values in the EK-BIO literature. For example, Wu *et al.* (2007) and Acar *et al.* (1997) reported k_e values of 2.5×10^{-9} m^2 V^{-1} s^{-1} and 4.6×10^{-9} m^2 V^{-1} s^{-1}, respectively. Second, a high f_{OC} can result in increased retardation that could decrease the toluene transport by electroosmosis below a threshold that makes biodegradation important (in these experiments, 0.066 mg l^{-1} h^{-1}). However, a high sediment f_{OC} can also impede bioremediation, by decreasing the

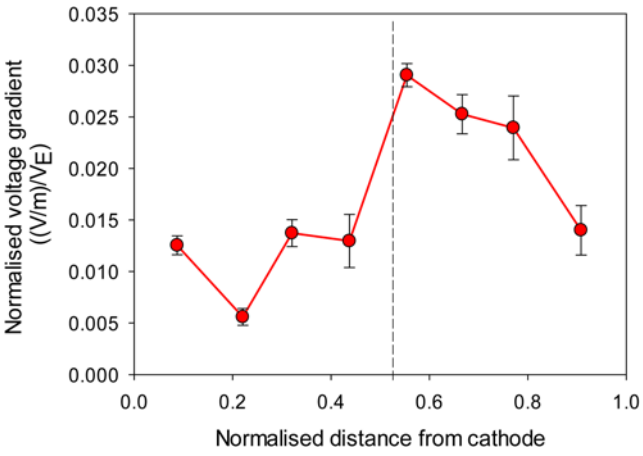

Fig. 9. Voltage gradient across the sediment section normalized to the voltage between electrodes (V_E) for Rig D. Error bars represent one standard deviation from the mean of four time points after the baseline. Dashed line indicates the location of the high-*K*–low-*K* interface.

bioavailability of the contaminant. In these experiments, the reported f_{OC} value 0.0016 allowed electroosmotic removal of 64, 71 and 57% of the toluene mass over 100 h in Rig A, C and D, respectively.

Implications for field applications

These findings indicate that in situations where the contaminant removal rate from a low-*K* zone by electroosmosis is high there will be an increased flux of contaminants into a host high-*K* material. Therefore, in these scenarios it would be more effective to focus bioremediation efforts (e.g. point of amendment addition) within the high-*K* zone. This could be beneficial to the bioremediation process. First, mixing of bacteria, contaminants and electron acceptors by advection and dispersion will be more effective in the high-*K* material. This reduces the mass-transfer limitations on biodegradation of contaminants (Simoni *et al.* 2001). Second, microbial abundance in fine-grained sediments is limited owing to narrow pore sizes (Rebata-Landa and Santamarina 2006). In these settings without the application of EK microbes are less motile and mass transfer is controlled by diffusion. Thus, in high-*K* zones where pore spaces are larger microbes may be in greater abundance and the conditions more conducive to bioremediation. Third, the presence of low-*K* zones facilitates greater mixing in the high-*K* host material, owing to disruption in the advective flowlines downgradient of the low-*K* zone (Bauer *et al.* 2009).

The method of bioremediation applied within the high-*K* zone could include either natural attenuation or biostimulation. Natural attenuation would be suitable if no immediate intensive remediation action was required and the background supply of electron acceptors in the high-*K* material was sufficient for biodegradation. Alternatively, biostimulation could be applied where electron acceptors or nutrients are introduced to support biodegradation. A similar concept was applied at field scale by Godschalk and Lageman (2005), who developed an EK-biofence to disperse electron donors and limiting nutrients from amendment wells to initiate biodegradation of Perchloroethylene (PCE) downgradient of the contaminant source. If there was a sensitive receptor downgradient, a hydraulic containment system could be installed to extract the contaminants released into the high-*K* zone. This is similar to the field-scale problem discussed by Gill *et al.* (2016*b*). Typically, the amount of contaminant recovered in these systems decreases over time, but is not necessarily representative of the reduction in contaminant mass still sequestered within the aquifer (USEPA 1994). EK could therefore be used to enhance the extraction of contaminants by hydraulic barrier systems.

Conclusions

This research has important implications for the application of EK-BIO in physically heterogeneous settings. Experimental data show that, under the conditions tested, electroosmosis is the most effective mechanism for contaminant removal from a low-*K* zone compared with diffusion and biodegradation. Further analysis indicated that for biodegradation to become the dominant removal mechanism the controlling parameters for contaminant electroosmotic flow velocity would need to be reduced (i.e. voltage gradient, electroosmotic permeability and sediment f_{OC}). Our initial hypothesis was that EK would enhance *in situ* bioremediation of toluene by increasing the supply of electron acceptors for biodegradation of toluene within a low-*K* zone, in which supply of electron acceptors by advection was poor. This research suggests that EK can indeed enhance *in situ* biodegradation under physically heterogeneous conditions and that a potential driving mechanism could be the electroosmotic movement of toluene out of the low-*K* zone into the high-*K* zone, where *in situ* biodegradation can more readily occur. Overall, this work provides evidence to re-evaluate the mechanism for most effective EK-BIO applications and aids the design of field-based systems that couple EK with bioremediation in physically heterogeneous settings to achieve the greatest *in situ* treatment.

Acknowledgements This work was completed while R.T.G. held a UK Engineering and Physical Sciences Research Council CASE studentship with Shell Global Solutions (UK) Ltd.

Author contributions **RTG**: formal analysis (lead), methodology (lead), writing – original draft (lead), writing – review & editing (lead); **ST**: supervision (lead), writing – original draft (supporting), writing – review & editing (supporting); **MJH**: supervision (supporting), writing – original draft (supporting), writing – review & editing (supporting); **JWS**: supervision (supporting), writing – original draft (supporting), writing – review & editing (supporting).

Funding This work was completed while the first author held a UK Engineering and Physical Sciences Research Council CASE studentship with Shell Global Solutions (UK) Ltd.

Data availability The datasets generated during and/or analysed during the current study are available in the White Rose Online repository, http://etheses.whiterose.ac.uk/12712/

Scientific editing by Jane Dottridge; Gary Wealthall

References

Acar, Y.B. and Alshawabkeh, A.N. 1993. Principles of electrokinetic remediation. *Environmental Science and Technology*, **27**, 2638–2647, https://doi.org/10.1021/es00049a002

Acar, Y.B., Rabbi, M.F. and Ozsu, E.E. 1997. Electrokinetic Injection of Ammonium and Sulfate Ions into Sand and Kaolinite Beds. *Journal of Geotechnical and Geoenvironmental Engineering*, **123**, 239–249, https://doi.org/10.1061/(ASCE)1090-0241(1997)123:3(239)

Anders, H.J., Kaetzke, A., Kampfer, P., Ludwig, W. and Fuchs, G. 1995. Taxonomic position of aromatic-degrading denitrifying pseudomonad strains K 172 and KB 740 and their description as new members of the genera *Thauera*, as *Thauera aromatica* sp. nov., and *Azoarcus*, as *Azoarcus evansii* sp. nov., respectively, members of the beta subclass of the Proteobacteria. *International Journal of Systematic and Evolutionary Microbiology*, **45**, 327–333, https://doi.org/10.1099/00207713-45-2-327

Bauer, R.D., Rolle, M. *et al.* 2009. Enhanced biodegradation by hydraulic heterogeneities in petroleum hydrocarbon plumes. *Journal of Contaminant Hydrology*, **105**, 56–68, https://doi.org/10.1016/j.jconhyd.2008.11.004

Bowers, R.L. and Smith, J.W.N. 2014. Constituents of potential concern for human health risk assessment of petroleum fuel releases. *Quarterly Journal of Engineering Geology and Hydrogeology*, **47**, 363–372, https://doi.org/10.1144/qjegh2014-005

Bruell, C.J., Segall, B.A. and Walsh, M.T. 1992. Electroosmotic Removal of Gasoline Hydrocarbons and TCE From Clay. *Journal of Environmental Engineering*, **118**, 68–83, https://doi.org/10.1061/(ASCE)0733-9372(1992)118:1(68)

British Standards Institute 1990. BS 1377-3:1990: *Methods of test for soils for civil engineering purposes* - Part 3: Chemical and electro-chemical tests. BSI, London.

CL:AIRE 2014. *An illustrated handbook of LNAPL transport and fate in the subsurface*. CL:AIRE.

Delle Site, A. 2001. Factors Affecting Sorption of Organic Compounds in Natural Sorbent/Water Systems and Sorption Coefficients for Selected Pollutants. A Review. *Journal of Physical and Chemical Reference Data*, **30**, 187–439, https://doi.org/10.1063/1.1347984

Fetter, C. 2001. *Applied Hydrogeology*, 4th edn. Prentice Hall, Upper Saddle River, NJ.

Gill, R.T. 2016. *Electrokinetic-enhanced migration of solutes for improved bioremediation in heterogeneous granular porous media*. PhD thesis, University of Sheffield.

Gill, R.T., Harbottle, M.J., Smith, J.W.N. and Thornton, S.F. 2014. Electrokinetic-enhanced bioremediation of organic contaminants: a review of processes and environmental applications. *Chemosphere*, **107**, 31–42, https://doi.org/10.1016/j.chemosphere.2014.03.019

Gill, R.T., Thornton, S.F., Harbottle, M.J. and Smith, J.W.N. 2015. Electrokinetic Migration of Nitrate Through Heterogeneous Granular Porous Media. *Groundwater Monitoring & Remediation*, **35**, 46–56, https://doi.org/10.1111/gwmr.12107

Gill, R.T., Thornton, S.F., Harbottle, M.J. and Smith, J.W. 2016*a*. Effect of physical heterogeneity on the electromigration of nitrate in layered granular porous media. *Electrochimica Acta*, **199**, 59–69, https://doi.org/10.1016/j.electacta.2016.02.191

Gill, R.T., Thornton, S.F., Harbottle, M.J. and Smith, J.W. 2016*b*. Sustainability assessment of electrokinetic bioremediation compared with alternative

remediation options for a petroleum release site. *Journal of Environmental Management*, **184**, 120–131, https://doi.org/10.1016/j.jenvman.2016.07.036

Godschalk, M.S. and Lageman, R. 2005. Electrokinetic Biofence, remediation of VOCs with solar energy and bacteria. *Engineering Geology*, **77**, 225–231, https://doi.org/10.1016/j.enggeo.2004.07.013

Hansen, B.H., Nedergaard, L.W., Ottosen, L.M., Riis, C. and Broholm, M.M. 2015. Experimental design for assessment of electrokinetically enhanced delivery of lactate and bacteria in 1,2-cis-dichloroethylene contaminated limestone. *Environmental Technology & Innovation*, **4**, 73–81, https://doi.org/10.1016/j.eti.2015.04.006

Hiscock, K. 2005. *Hydrogeology: Principles and Practice*. Blackwell, Oxford.

Huang, D., Guo, S., Li, T. and Wu, B. 2013. Coupling Interactions between Electrokinetics and Bioremediation for Pyrene Removal from Soil under Polarity Reversal Conditions. *CLEAN – Soil, Air, Water*, **41**, 383–389, https://doi.org/10.1002/clen.201200079

Jenneman, G.E., McInerney, M.J., Crocker, M.E. and Knapp, R.M. 1986. Effect of Sterilization by Dry Heat or Autoclaving on Bacterial Penetration through Berea Sandstone. *Applied and Environmental Microbiology*, **51**, 39–43, https://doi.org/10.1128/AEM.51.1.39-43.1986

Lavanchy, P.M. 2008. *Microbial community metabolic concurrence involved in toluene degradation: Effect of oxygen availability on catabolic gene expression of aerobic and anaerobic toluene degrading bacteria*. PhD thesis, Friedrich-Schiller University Jena.

Luo, Q., Zhang, X., Wang, H. and Qian, Y. 2005. Mobilization of phenol and dichlorophenol in unsaturated soils by non-uniform electrokinetics. *Chemosphere*, **59**, 1289–1298, https://doi.org/10.1016/j.chemosphere.2004.11.043

Mao, X., Wang, J. *et al.* 2012. Electrokinetic-enhanced bioaugmentation for remediation of chlorinated solvents contaminated clay. *Journal of Hazardous Materials*, **213–214**, 311–317, https://doi.org/10.1016/j.jhazmat.2012.02.001

Rabbi, M.F., Clark, B., Gale, R.J., Ozsu-Acar, E., Pardue, J. and Jackson, A. 2000. *In situ* TCE bioremediation study using electrokinetic cometabolite injection. *Waste Management*, **20**, 279–286, https://doi.org/10.1016/S0956-053X(99)00329-3

Rebata-Landa, V. and Santamarina, J.C. 2006. Mechanical limits to microbial activity in deep sediments. *Geochemistry, Geophysics, Geosystems*, **7**, https://doi.org/10.1029/2006GC001355

Reynolds, D.A., Jones, E.H., Gillen, M., Yusoff, I. and Thomas, D.G. 2008. Electrokinetic migration of permanganate through low-permeability media. *Ground Water*, **46**, 629–637, https://doi.org/10.1111/j.1745-6584.2008.00415.x

Rivett, M.O., Buss, S.R., Morgan, P., Smith, J.W. and Bemment, C.D. 2008. Nitrate attenuation in groundwater: a review of biogeochemical controlling processes. *Water Research*, **42**, 4215–4232, https://doi.org/10.1016/j.watres.2008.07.020

Saichek, R.E. and Reddy, K.R. 2005. Surfactant-enhanced electrokinetic remediation of polycyclic aromatic hydrocarbons in heterogeneous subsurface environments. *Journal of Environmental Engineering and Science*, **4**, 327–339, https://doi.org/10.1139/s04-064

Simoni, S.F., Schäfer, A., Harms, H. and Zehnder, A.J.B. 2001. Factors affecting mass transfer limited biodegradation in saturated porous media. *Journal of Contaminant Hydrology*, **50**, 99–120, https://doi.org/10.1016/S0169-7722(01)00099-7

Song, X. and Seagren, E.A. 2008. *In situ* bioremediation in heterogeneous porous media: dispersion-limited scenario. *Environmental Science and Technology*, **42**, 6131–6140, https://doi.org/10.1021/es0713227

Tatti, F., Papini, M.P., Sappa, G., Raboni, M., Arjmand, F. and Viotti, P. 2018. Contaminant back-diffusion from low-permeability layers as affected by groundwater velocity: A laboratory investigation by box model and image analysis. *Science of The Total Environment*, **622–623**, 164–171, https://doi.org/10.1016/j.scitotenv.2017.11.347

Thornton, S.F., Lerner, D.N. and Tellam, J.H. 1995. *The Technical Aspects of Controlled Waste Management: Laboratory Studies of Landfill Leachate–Triassic Sandstone Interactions*, Department of the Environment.

Thornton, S.F., Morgan, P.M. and Rolfe, S.A. 2016. Bioremediation of hydrocarbons and chlorinated solvents in groundwater. *In*: McGenity, T.J., Timmis, K.N. and Nogales, B. (eds) *Protocols for Hydrocarbon and Lipid Microbiology*. Springer, Berlin, 1–54.

USEPA. 1994. *Methods for Monitoring Pump and Treat Performance*. Report **EPA/625/R-95/005**. USEPA, Washington, DC.

Wu, M.Z., Reynolds, D.A., Fourie, A., Prommer, H. and Thomas, D.G. 2012*a*. Electrokinetic *in situ* oxidation remediation: assessment of parameter sensitivities and the influence of aquifer heterogeneity on remediation efficiency. *Journal of Contaminant Hydrology*, **136–137**, 72–85, https://doi.org/10.1016/j.jconhyd.2012.04.005

Wu, M.Z., Reynolds, D.A., Prommer, H., Fourie, A. and Thomas, D.G. 2012*b*. Numerical evaluation of voltage gradient constraints on electrokinetic injection of amendments. *Advances in Water Resources*, **38**, 60–69, https://doi.org/10.1016/j.advwatres.2011.11.004

Wu, X., Alshawabkeh, A.N., Gent, D.B., Larson, S.L. and Davis, J.L. 2007. Lactate Transport in Soil by DC Fields. *Journal of Geotechnical and Geoenvironmental Engineering*, **133**, 1587–1596, https://doi.org/10.1061/(ASCE)1090-0241(2007)133:12(1587)

Wu, X., Gent, D.B., Davis, J.L. and Alshawabkeh, A.N. 2012*c*. Lactate Injection by Electric Currents for Bioremediation of Tetrachloroethylene in Clay. *Electrochimica Acta*, **86**, 157–163, https://doi.org/10.1016/j.electacta.2012.06.046